Boundary-Conditions, Temperatures, and Stress-Intensity Factors under Arbitrary Thermal Transients via the Inverse Route

A.E. Segall and J. Meeker
Engineering Science and Mechanics
The Pennsylvania State University
University Park, PA 16802 Email: aesegall@psu.edu

ABSTRACT A common threat to components is thermal shock from operational steady-state or transient thermal-states; an analysis of this type of problem ultimately requires the determination of stress-intensity factors (SIF). For direct problems where all boundary conditions are known, the procedure is relatively straightforward and mathematically tractable. Although more practical from a measurement standpoint, the inverse problem where the boundary conditions must be determined from remotely determined temperature and/or flux data is ill-posed and inherently sensitive to errors in the data. Despite these difficulties, the inverse problem can on-fact be solved using a least-squares determination of polynomial coefficients based on a generalized direct-solution to the Heat Equation. Once the unknown surface temperature-history was determined, the resulting polynomial was used with the generalized direct solution to determine the temperature and stress distributions as a function of time. For a semi-infinite slab with both edge- and surface-cracks, excellent agreement was seen with known solutions. Given the versatility of the polynomial solutions advocated, the method appears well suited for many thermal scenarios provided the analysis is restricted to the time interval used to determine the polynomial and the thermophysical properties that do not vary with temperature. The method can also be implemented as part of a finite-element solution for more complex geometries where closed-form solutions do not exist.

INTRODUCTION

Thermal shock is a common problem encountered in many applications ranging from aerospace to manufacturing. Regardless of the application and underlying cause, thermal-shock failures are expensive because of the equipment and repair costs, as well as the associated time and resources expended. Given these concerns, a large number of studies of thermal shock have been conducted over the years. Most have concentrated on the thermoelastic stress-states and the resulting propensity for cracking and failure [1], [2], [3], [4], [5]. However, these approaches were generally "macroscopic" in that average fracture strengths or Weibull based statistical parameters were used without any consideration of individual flaws. While certainly useful for the safe and efficient use of many materials such as ceramics, it does not help with the analysis of individual defects that may grow over time as a result of thermomechanical fatigue. In order to help analyze individual flaws, stress-intensity factor (SIF) solutions have evolved over the years for various crack geometries and thermal loading scenarios. In fact, for the analysis of plates and slabs under a thermal shock, numerous solutions can be found [6], [7], [8], [9], [10], [11], [12]. However, a review of these stress intensity solutions reveals that the transient thermal loading is usually restricted to either a step or linear function of time to help keep the mathematics tractable. Generally, most thermal shocks are asymptotic in their rise and/or decay and cannot be reasonably modeled as instantaneous or linear as already shown [2],[3], [13]. Consequently, the actual time, magnitude, and/or location of the maximum stress intensity may vary significantly from an overly conservative (and potentially unrealistic prediction based on step loading scenarios. As such, more realistic assessments of the boundary conditions and their temporal dependencies is required to avoid thermal-shock failures.

For a more arbitrary (and realistic) thermal-loading scenario, the weight function approach [14] represents a powerful method for the direct calculation of SIF's. However, the use of weight functions requires a detailed understanding of the tensile stresses acting along the crack front at any given instant of time. This in-turn requires an analysis of the stress distribution for each loading case over the entire time interval of interest. While the advent of finite-element analysis (FEA) has made this possible (and increasingly common), the process can be extremely tedious for transient studies because each time-interval and its associated stress-state acting along the crack-face must be quasi-statically captured and "fit" to some form of a function such as a polynomial. Once determined, this relationship can then be readily integrated with the weight function to determine the SIF for any given instant.

Given these limitations and the need to realistically address the time-dependent nature of thermal shock, a study was undertaken to derive transient stress intensity factors for a plate subjected to an arbitrary thermal shock via the inverse route. The results presented herein show how generalized SIF solutions are possible (both direct and inverse) if the materials thermal and elastic properties are assumed constant and a known surface temperature history can be reasonably described by a polynomial.

ANALYTICAL CONSIDERATIONS

For the finite thickness slab of thickness, h, shown in Fig. 1, the solution for a unit surface load is [15],[16]:

$$\Phi(x,t) = T_s\left[1 - \sum_{k=1}^{\infty} \Psi_k e^{-b_k^2 t}\right] \tag{1}$$

$$\Psi_k = A_k \cos\left(Q_k \frac{x-h}{h}\right) \tag{2}$$

$$A_k = \frac{4(-1)^{k+1}}{\pi(2k-1)} \tag{3}$$

$$Q_k = \frac{\pi(2k-1)}{2} \tag{4}$$

$$b_k^2 = \frac{DQ_k^2}{h^2} \tag{5}$$

where T is the temperature, t is time, x is the coordinate from the thermally loaded surface, and D is the thermal diffusivity that is assumed to be independent of temperature. Once determined, the resulting step response for a unit temperature change can also be used as a kernel with Duhamel's relationship [17]:

$$T(x,t) = \int_0^t \frac{\partial T_s(0,\tau)}{\partial \tau} \Phi(x, t-\tau) d\tau = T_s * \Phi(x,t) \tag{6}$$

to determine a response T(x,t), to an arbitrary surface (x/h=0) excitation $T_s(t)$. Using this formulation, the next step is to solve the resulting Volterra Equation while maintaining some degree of generalization for the thermal load. One way to achieve both goals is through the use of a relatively versatile polynomial containing both integral-and half-order terms:

$$T_s(t) = a_0 + a_1 t^{\frac{1}{2}} + a_2 t + a_3 t^{\frac{3}{2}} + \cdots = \sum_{n=0}^{\infty} a_n t^{\frac{n}{2}} \tag{7}$$

where a_n represent polynomial coefficients determined using least squares methods. Given the form of Eqs (1, 6, and 7), the transient response to a system initially at a temperature of zero under a generalized polynomial excitation [18] becomes:

$$T(x,t) = \sum_{n=1}^{N} a_n \left[t^{n/2} - \frac{n}{2}\delta_n(x,t)\right] \tag{8}$$

where the response terms can be expressed as:

$$\delta_{2j-1}(x,t) = \frac{(-1)^{j+2}}{2^{j-1}}\zeta(j-1, 2j-3)\sum_{k=1}^{\infty}\frac{\Psi_k \Omega_k}{b_k^{2j-2}} + \frac{2}{\pi}\tan^{-1}\left[e^{10}(j-1)\right]\sum_{i=0}^{j-2}\left[(-1)^i \frac{t^{\frac{2(j-i)-3}{2}}}{2^i}\zeta(i, 2j-3)\sum_{k=1}^{\infty}\frac{\Psi_k}{b_k^{2(i+1)}}\right] \tag{9}$$

$$\delta_{2j}(x,t) = (-1)^j \chi(j-1, j-1)\sum_{k=1}^{\infty}\frac{\Psi_k e^{-b_k^2 t}}{b_k^{2j}} + \sum_{i=0}^{j-1}\left[(-1)^i t^{j-i-1}\chi(i, j-1)\sum_{k=1}^{\infty}\frac{\Psi_k}{b_k^{2(i+1)}}\right] \tag{10}$$

with the subscript integer set as j=1,2,3…N and the reoccurring functions $\chi(\eta,\lambda)$ and $\xi(\eta,\lambda)$ defined as:

$$\chi(\eta,\lambda) = \frac{\lambda!}{(\lambda-\eta)!} \qquad \zeta(\eta,\lambda) = \frac{2^{\eta}\Gamma(\lambda/2+1)}{\Gamma(\lambda/2+1-\eta)} \tag{11}$$

where Γ is the Gamma function. Additionally, the use of half-order terms by the polynomial results in a reoccurring function that can be approximated as

$$\Omega_k(t) \approx \frac{\mathrm{Ln}(2)}{t}\sum_{m=1}^{10}\varphi_m\left[\frac{\sqrt{\pi}}{\sqrt{s_m^*}\left(s_m^*+b_k^2\right)}\right] \quad \text{where} \quad s_m^* = \frac{\mathrm{Ln}(2)}{t}m \tag{15}$$

with the series coefficients φ_m, listed in Table 1.

INVERSE CALCULATIONS

While Eq. (8) is clearly a direct solution of the problem with a know boundary condition as a function of time, its form can also be used for a more generalized solution of the corresponding inverse problem [19]. In fact, a generalized inverse solution is possible by fitting temperatures, υ obtained at x to a new polynomial with the coefficients a_1, a_2,…a_n that satisfy:

$$\begin{bmatrix} \frac{\partial T_n}{\partial t}*\Phi(x,t_1) & \frac{\partial T_{n+1}}{\partial t}*\Phi(x,t_1) & \dots & \frac{\partial T_N}{\partial t}*\Phi(x,t_1) \\ \frac{\partial T_n}{\partial t}*\Phi(x,t_2) & \frac{\partial T_{n+1}}{\partial t}*\Phi(x,t_2) & \dots & \frac{\partial T_N}{\partial t}*\Phi(x,t_2) \\ \vdots & \vdots & & \vdots \\ \frac{\partial T_n}{\partial t}*\Phi(x,t_N) & \frac{\partial T_{n+1}}{\partial t}*\Phi(x,t_N) & \dots & \frac{\partial T_N}{\partial t}*\Phi(x,t_N) \end{bmatrix}\begin{bmatrix} a_n \\ a_{n+1} \\ \vdots \\ a_N \end{bmatrix} = \begin{bmatrix} \upsilon(x,t_n) \\ \upsilon(x,t_{n+1}) \\ \vdots \\ \upsilon(x,t_N) \end{bmatrix} \tag{16}$$

Once the coefficients are determined, the direct solution obtained via Eq. (1) can then be used to determine the temperature distribution throughout the solid. Hence, the analytical solution of the inverse problem boils down to determining the more tractable direct problem and using the solution to determine the coefficients for the unknown boundary condition in a least-squares sense. While any function or combination of functions can be used to describe a time-varying temperature, a polynomial represents a relatively straightforward method. Fig. 2 shows a polynomial fit to a linear down-shock followed by a constant soak period that was used earlier [8] for the semi-numerical evaluation of thermal-shock stress intensity factors. As shown in the figure, the polynomial was able to reasonably fit the overall form of the temperature history with minimal polynomial oscillations; while this fit illustrates the potential pitfalls of using polynomials (especially to model linear segments and/or sharp corners), it also shows how the least-squares process can mimic what should in reality, be a smoother, asymptotic temperature history. Fig. 2 also shows the excellent Inverse prediction of the surface boundary-condition via the least squares method from the remote temperature obtained at the opposing surface at x/h=1.

THERMOELASTIC STRESSES

After the transient temperature distribution was determined as a function of the polynomial coefficients, thermoelasticity theory was used to determine the resulting stress-states. For a planar geometry, the crack-opening stress was determined by the following generalized relationship:

$$\sigma_y = \frac{\alpha E}{(1-\nu)}\left[\frac{4h-6x}{h^2}\int_0^h T(x,t)dx + \frac{12x-6h}{h^3}\int_0^h xT(x,t)dx - T(x,t)\right] \tag{17}$$

where E is the elastic modulus, ν is Poisson's ratio, and α is the coefficient of thermal expansion. Substitution of the transient temperature distribution resulted in the following relationship for the crack-opening thermal stress.

$$\sigma_y = \frac{\alpha E}{(1-\nu)}\left[\frac{4h-6x}{h^2}\ \lambda 1\ +\ \frac{12x-6h}{h^3}\ \lambda 2\ -\ T(x,t)\right] \tag{18}$$

In Eq. (18), the zeroth and first temperature moments are defined as:

$$\lambda 1 = \sum_{n=1}^{N} a_n h\left[t^{\frac{n}{2}} - \frac{n}{2}\bar{\delta}_n(t)\right] \quad \text{and} \quad \lambda 2 = \sum_{n=1}^{N} a_n \frac{h^2}{2}\left[t^{\frac{n}{2}}\ -\ \frac{n}{2}\bar{\bar{\delta}}_n(t)\right] \tag{19}$$

where the terms $\bar{\delta}_n$ and $\bar{\bar{\delta}}_n$ represent the response functions given by Eqs. (9 or 10), respectively with Ψ_k replaced by the Equations below:

$$\bar{\Psi}_k = \frac{A_k}{Q_k}\ \sin(Q_k) \quad \text{and} \quad \bar{\bar{\Psi}}_k = \frac{2A_k}{Q_k^2}\ \left[1-\cos(Q_k)\right] \tag{20}$$

All other terms and variables are as previously defined. Fig. 3 shows a comparison of the resulting stresses for the linear portion of the loading for various values of non-dimensional time and axial location away from the exposed surface. As shown in the figure, reasonable agreement is found for the thermoelastic response of the slab to the imposed down-shock.

STRESS INTENSITY CALCULATIONS

With the thermoelastic stress-state approximated for an arbitrary thermal shock, the transient mode-I stress intensity factors, K_I were then calculated using a weight-function approach:

$$K_I = \int_o^a w(x)\ \sigma(x)\ dx \tag{21}$$

where w(x) is the weight function and the variable a, represents the crack length (Fig. 1). For a planar geometry such as a slab or plate, the weight function has been shown to assume the following form [9]:

$$w(x) = \frac{1}{\sqrt{2\pi(a-x)/h}}\left[1 + M_1\ (1-x/a) + M_2\ (1-x/a)^2\right] \tag{22}$$

where the functions M_1 and M_2 reflect the crack geometry. Given this form of the weight function and the previously defined the thermal stress-state, the mode-I stress intensity factor, K_I for an arbitrary thermal shock becomes:

$$K_I = \frac{E\alpha}{(1-\nu)}\left[\psi 1\ \ \lambda 1 + \psi 2\ \ \lambda 2 - \sum_{n=1}^{N} a_n\left[\psi 3\ \ t^{\frac{n}{2}} - \frac{n}{2}\delta_n'(t)\right]\right] \tag{23}$$

where

$$\psi 1 = -\frac{4\sqrt{\frac{2a}{\pi h}}}{105h}\left[3a\ (35 + 7M_1 + \ 3M_2) - 7h\ (5M_1 + 3\ (5 + M_2))\right] \tag{24}$$

$$\psi 2 = -\frac{2\sqrt{\frac{2a}{\pi h}}}{35h^2}\left[4a\ (35 + 7M_1 + \ 3M_2) - 7h\ (5M_1 + 3\ (5 + M_2))\right] \tag{25}$$

$$\psi 3 = -\frac{\sqrt{\frac{2a}{\pi h}}}{15}\left[h\ (5 + M_1 + 3\ (5 + M_2))\right] \tag{26}$$

$$\psi 4_k = \frac{1}{Q_k(1/h)^{3/2}}\left[\sqrt{\frac{Q_k}{h}}\ \ (\cos(\theta_k)C(\gamma_k) - S(\gamma_k)\sin(\theta_k))\right] \tag{27}$$

$$\psi 5_k = \frac{1}{2Q_k^2\left(\frac{a}{t}\right)^{3/2}}\left[\sqrt{a}M_1\ \left[\sqrt{\frac{2a}{\pi}}\ \ Q_k \mathrm{Sin}(Q_k) - h\left\{\sqrt{\frac{Q_k}{h}\left[\cos(\theta_k)S(\gamma_k)\ +\ C(\gamma_k)\sin(\theta_k)\right]}\right\}\right]\right] \tag{28}$$

$$\psi 6_k = \frac{1}{4Q_k^3 a^2\left(\frac{1}{h}\right)^{3/2}}\ \ M_2\left[3h^2\sqrt{\frac{Q_j}{h}}(\sin(\theta_k)S(\gamma_k) - C(\gamma_k)\cos(\theta_k)) + \sqrt{\frac{2a}{\pi}}\ \ Q_k\left(3h\cos(Q_k) + 2aQ_k\sin(Q_k)\right)\right] \tag{29}$$

where δ'_n represent the response functions given by Eqs. (9 or 10), respectively with Ψ_k now replaced by ψ_k from below:

$$\psi_k = A_k \left(\psi 4_k + \psi 5_k + \psi 6_k \right) \tag{30}$$

Within the preceding equations, the recurring parameters γ_k and θ_k are defined below and C(z) and S(z) representing the Cosine- and Sine-based Fresnel Integrals, respectively:

$$\gamma_k = \sqrt{\frac{2aQ_k}{\pi h}} \quad \text{and} \quad \theta_k = Q_k \left(1 - \frac{a}{h} \right) \tag{31}$$

The next phase of the analysis was directed at calculating stress intensity factors using the newly derived relationships. Since solutions are readily available [8] for edge-cracked plates subjected to the down-shock shown in Fig. 2, comparative calculations were undertaken using graphically interpolated data. For such an edge-cracked geometry, the two terms M_1 and M_2 used in the weight-function were defined as:

$$M_1 = 0.6147 + 17.1844 \left(\frac{a}{h} \right)^2 + 8.7822 \left(\frac{a}{h} \right)^6 \quad \text{and} \quad M_2 = 0.2502 + 3.2899 \left(\frac{a}{h} \right)^2 + 70.0444 \left(\frac{a}{h} \right)^6 \tag{32}$$

When these functions were used along with the stress intensity solution just derived and compared to the earlier numerical study, excellent agreement was observed for various crack-to-thickness ratios as shown by Fig. 4. The relatively small differences observed throughout the thermal, stress, and SIF calculations may be attributed in-part, to the fact that the earlier study [8] used numerical integration for portions of their study to determine final values. Another factor is the smoothing influence of the polynomial fit used to simulate the down-shock. Since most down shocks should not exhibit abrupt behaviors, the smoothing influence of the polynomial may actually represent an advantage. Regardless of the form of the down-shock, the analysis should always be restricted to the time interval used to describe the polynomial to avoid the risk of it going astray.

CONCLUSIONS

An approximate inverse solution was derived that allows the calculation of the thermal transients caused by an arbitrary surface loading on a finite-thickness slab. The arbitrary nature of the thermal loading was allowed through the use of a versatile polynomial that employed integral-and half-order terms. When this solution was used in conjunction with a weight-function for an edge-cracked slab, stress intensity factor solutions were obtained that show excellent agreement with earlier numerical studies. The method appears will suited for complicated thermal shocks provided the analysis is restricted to the time interval used to determine the polynomial.

REFERENCES

1. Vedula, V.R., Green, D.J., Hellmann, J.R., and Segall, A.E., "Test Methodology for the Thermal Shock Characterization of Ceramics," *Journal of Materials Science*, Vol. 33, 1999, pp. 5427-5432.

2. Segall, A.E., Hellmann, J.R., and Modest, M.F., "Analysis of Gas-Fired Ceramic Radiant Tubes During Transient Heating," *ASTM Journal of Testing and Evaluation*, Vol. 19, 1991, pp. 454-460.

3. Segall, A.E., Hellmann, J.R., and Tressler, R.E., "Thermal Shock and Fatigue Behavior of Ceramic Tubes," *Proceedings of the 10th Biennial ASME Conference on Reliability, Stress Analysis, and Failure Prevention*, New Mexico, pp. 81-87, 1993.

4. Albrecht, W., "How Thickness and Materials Properties Influence Thermal-Stresses in Flat Plates and Cylinders," ASME paper G9-GT-107, 1969.

5. Hasselman, D.P.H., "Thermal Stress Resistance Parameters for Brittle Refractory Ceramics: A Compendium," *Bull. Amer. Ceram. Soc.*, Vol. 49, 1970, pp. 1033-1037.

6. Shiratori, M., Niyoshi, T. and Tanikawa, K., Stress Intensity Factor Handbook-Volume I. Pergamon Press, Oxford, 1987.

7. Shiratori, M., Niyoshi, T. and Tanikawa, K., Stress Intensity Factor Handbook-Volume II. Pergamon Press, Oxford, 1987.

8. El-Fattah, E., Rizk, A., and Radwan, S. F., "Fracture of a Plate under Transient Thermal Stresses," *J. Thermal Stresses*, Vol. 16, 1993, pp. 79-102.

9. Lee, K. Y. and Sim, K. B., "Thermal Shock Stress Intensity Factor by Bueckner's Weight Function Method," *Engineering Fracture Mechanics*, Vol. 37, 1990, pp. 799-804.

10. Emory, F., Walker, G. E., Jr. and Williams, J.A., "Green's Function for the Stress Intensity Factors of Edge Cracks and its Application to Thermal Stresses," *J. Basic Engineering*, Vol. 91, 1969, pp. 618-624.

11. Nied, H. F., "Thermal Shock in an Edge-Cracked Plate Subjected to Uniform Surface Heating," *Engineering Fracture Mech*. Vol. 26, 1987, pp. 239-246.

12. Y. W. Kim, J. H. Lee, and B. Yoo, "An analysis of stress intensity factors for thermal transient problems based on Green's function," *Engineering Fracture Mech*. Vol. 49, 1994, pp. 393-403.

13. Tu, J.J. and Segall, A.E., "Thermomechanical analysis of a complex, refractory tundish flow modifier during preheating," *Proceedings of the Unified International technical Conference on Refractories, 5th Biennial Worldwide Congress*, New Orleans, LA, 1997.

14. Bueckner, P., "Weight functions for the Notched Bar," *Z. Angew. Mathe. Mech*., Vol. 51, 1971, pp. 97-109.

15. Chen, S.H., "One-Dimensional Heat Conduction with Arbitrary Heating Rate," *Journal of Aerospace Sciences*, Vol. 28, 1961, pp. 336-337.

16. Austin, J.B., "Temperature Distribution in Solid Bodies during Heating or Cooling," *Journal of Applied Physics*, Vol. 3, 1932, pp.179-183.

17. Fodor, G., *Laplace Transforms in Engineering*, Akademiai Kiado, Budapest, 1965.

18. Segall, A.E., "Thermal Stresses in an Infinite Slab under an Arbitrary Thermal Shock," *ASME J. Applied Mechanics*, Vol. 70, 2003, pp. 779-782.

19. Segall, A.E., "Inverse Solutions for Determining Arbitrary Boundary-Conditions using a Least-Squares Approach," ASME Journal of Heat Transfer, Vol. 127, 2005 pp. 1403-1405.

Table 1 Gaver-Stehfest coefficients used for the approximation of the inverse Laplace Transform of the recurring integral.

m	φ_m
1	0.0833
2	-32.0833
3	1270.0008
4	-15623.6669
5	84244.1695
6	-236957.5129
7	375911.6923
8	-340071.6923
9	164062.5128
10	-32812.5026

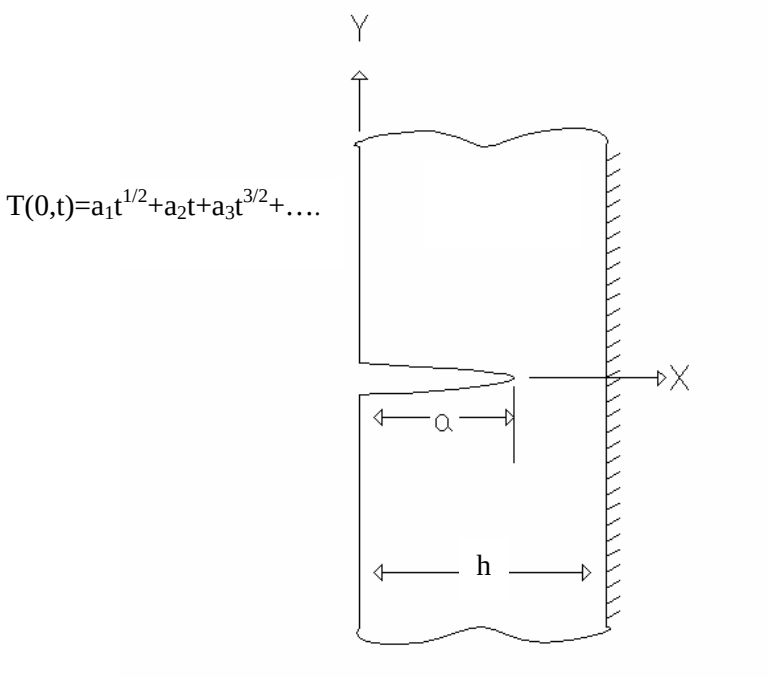

$T(0,t)=a_1t^{1/2}+a_2t+a_3t^{3/2}+\ldots$

Fig. 1 Slab geometry including crack-geometry and applied boundary conditions on both surfaces.

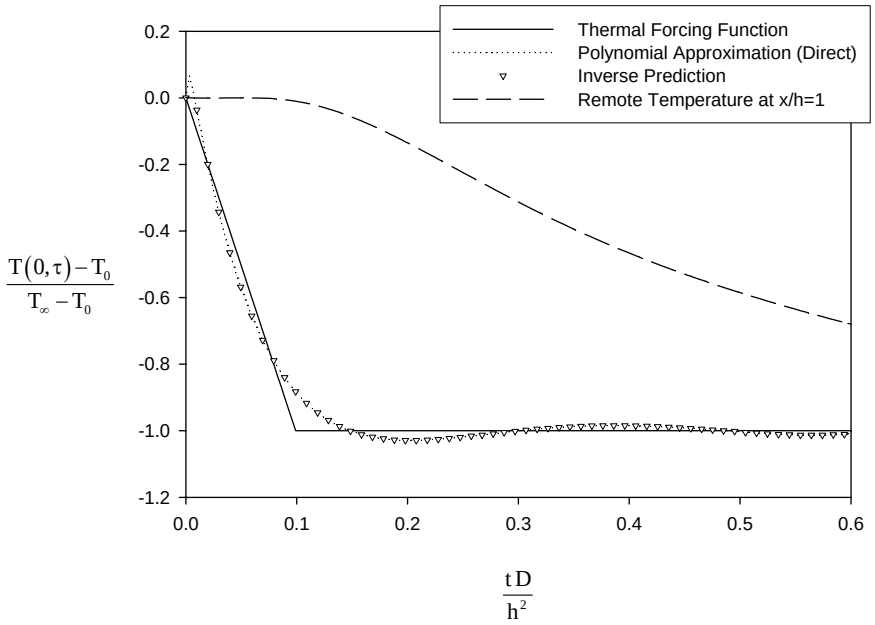

Fig. 2 Down-shock thermal scenario with approximating polynomial, the resulting and remote response at x/h=1, and the inverse prediction.

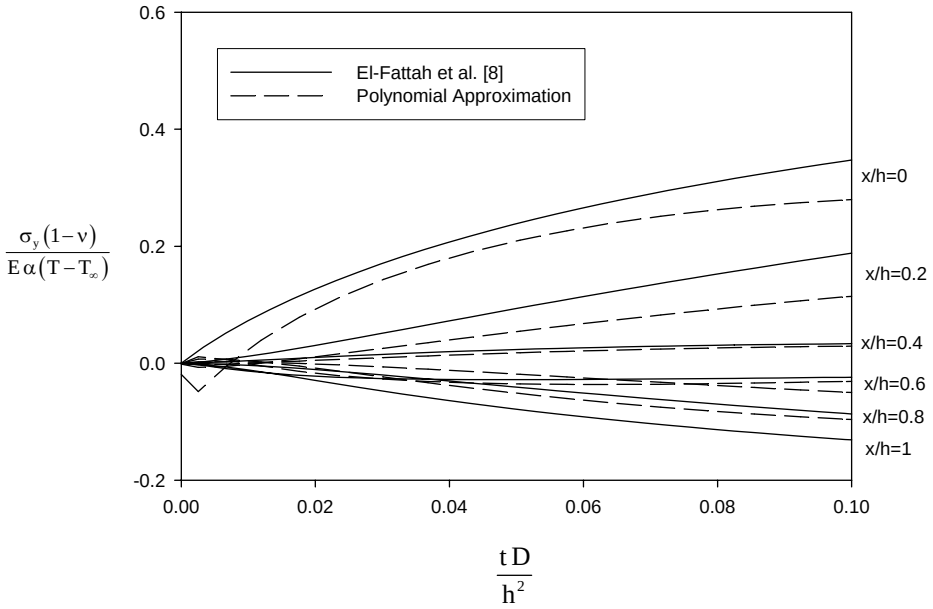

Fig. 3 Comparisons of transient, thermal-stresses calculated for various depths as a function of time for the down-shock.

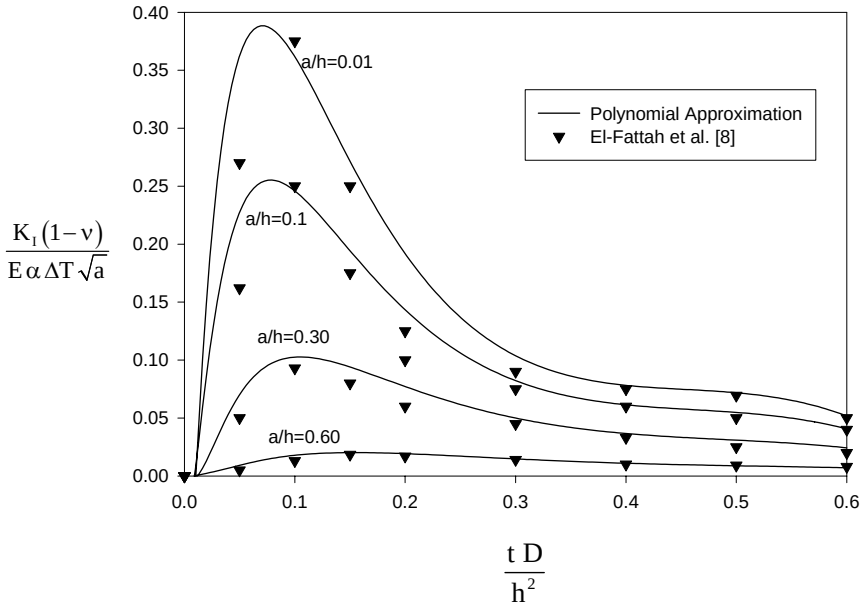

Fig. 4 Comparison of normalized, transient stress-intensity factors predictions for various crack sizes under the down-shock shown in Fig. 1.